

# Evaluating China's fossil-fuel CO<sub>2</sub> emissions from a comprehensive dataset of nine inventories

Pengfei Han<sup>1\*</sup>, Ning Zeng<sup>2\*</sup>, Tom Oda<sup>3</sup>, Xiaohui Lin<sup>4</sup>, Monica Crippa<sup>5</sup>, Dabo Guan<sup>6,7</sup>, Greet Janssens-Maenhout<sup>5</sup>, Xiaolin Ma<sup>8</sup>, Zhu Liu<sup>6,9</sup>, Yuli Shan<sup>10</sup>, Shu Tao<sup>11</sup>, Haikun Wang<sup>8</sup>, Rong Wang<sup>11,12</sup>, Lin Wu<sup>4</sup>, Xiao Yun<sup>11</sup>, Qiang Zhang<sup>13</sup>, Fang Zhao<sup>14</sup>, Bo Zheng<sup>15</sup>

<sup>1</sup>State Key Laboratory of Numerical Modeling for Atmospheric Sciences and Geophysical Fluid Dynamics, Institute of Atmospheric Physics, Chinese Academy of Sciences, Beijing, China

<sup>2</sup>Department of Atmospheric and Oceanic Science, and Earth System Science Interdisciplinary Center, University of Maryland, College Park, Maryland, USA

<sup>3</sup>Goddard Earth Sciences Research and Technology, Universities Space Research Association, Columbia, MD, United States

<sup>4</sup>State Key Laboratory of Atmospheric Boundary Layer Physics and Atmospheric Chemistry, Institute of Atmospheric Physics, Chinese Academy of Sciences, Beijing, China

<sup>5</sup>European Commission, Joint Research Centre (JRC), Directorate for Energy, Transport and Climate, Air and Climate Unit, Ispra (VA), Italy

<sup>6</sup>Department of Earth System Science, Tsinghua University, Beijing, China

<sup>7</sup>Water Security Research Centre, School of International Development, University of East Anglia, Norwich, UK

<sup>8</sup>State Key Laboratory of Pollution Control and Resource Reuse, School of the Environment, Nanjing University, Nanjing, China

<sup>9</sup>Tyndall Centre for Climate Change Research, School of International Development, University of East Anglia, Norwich, UK

<sup>10</sup>Energy and Sustainability Research Institute Groningen, University of Groningen, Groningen 9747 AG, Netherlands

<sup>11</sup>Laboratory for Earth Surface Processes, College of Urban and Environmental Sciences, Peking University, Beijing, China

<sup>12</sup>Department of Environmental Science and Engineering, Fudan University, Shanghai, China

<sup>13</sup>Ministry of Education Key Laboratory for Earth System Modeling, Department of Earth System Science, Tsinghua University, Beijing, China

<sup>14</sup>Key Laboratory of Geographic Information Science (Ministry of Education), School of Geographic Sciences, East China Normal University, Shanghai, China

<sup>15</sup>Laboratoire des Sciences du Climat et de l'Environnement, CEA-CNRS-UVSQ, UMR8212, Gif-sur-Yvette, France

*Correspondence to:* Pengfei Han (pphan@mail.iap.ac.cn); Ning Zeng (zeng@umd.edu)

**Abstract.** China's fossil-fuel CO<sub>2</sub> ~~emissions~~-(FFCO<sub>2</sub>) emissions accounted for ~~about approximately~~ 28% of the global total FFCO<sub>2</sub> in 2016. An accurate estimate of China's FFCO<sub>2</sub> emissions is a prerequisite for global and regional carbon budget analyses and the monitoring of carbon emission reduction efforts. However, ~~large-significant~~ uncertainties and discrepancies exist in estimations of China's FFCO<sub>2</sub> ~~emissions estimations~~ due to a lack of detailed traceable emission factors (EF) and multiple statistical data sources. Here, we evaluated China's FFCO<sub>2</sub> emissions from nine<sup>9</sup> published global and regional emission datasets. These datasets show that the total emissions increased from 3.4 (3.0-3.7) in 2000 to 9.8 (9.2-10.4) Gt CO<sub>2</sub> yr<sup>-1</sup> in 2016. The variations in ~~their-these~~ estimates were ~~due~~ largely due to the different EF (0.491-0.746 t C per t of coal) and activity data. The large-scale patterns of gridded emissions showed a reasonable agreement with high emissions being

concentrated in major city clusters, and the standard deviation mostly ranged ~~from~~ 10-40% at ~~the~~ provincial level. However, patterns beyond the provincial scale ~~vary varied greatly significantly,~~ with the top 5% of ~~the~~ grid-level accounting for 50-90% of total emissions ~~for-in~~ these datasets. Our findings highlight the significance of using locally-measured EF for ~~the~~ Chinese coals. To reduce ~~the~~ uncertainty, we ~~call-on-the-enhancement-of~~ recommend using physical CO<sub>2</sub> measurements and use ~~them~~ these values for datasets validation, key input data sharing (e.g., point sources) and finer resolution validations at various levels.

**Keywords:** fossil-fuel CO<sub>2</sub> emissions, spatial disaggregation, emission factor, activity data, comprehensive dataset

## 1 Introduction

Anthropogenic emissions of carbon dioxide (CO<sub>2</sub>) is one of the major ~~contributions in accelerating accelerators of~~ global warming (IPCC, 2007). ~~The-g~~Global CO<sub>2</sub> emissions from fossil fuel combustion and industry processes increased to 36.23 Gt CO<sub>2</sub> yr<sup>-1</sup> in 2016, with a mean growth rate of 0.62 Gt CO<sub>2</sub> yr<sup>-1</sup> ~~per-year~~ over the last decade (Le Quéré et al., 2018). In 2006, China became the world's largest emitter of CO<sub>2</sub> (Jones, 2007). ~~The~~CO<sub>2</sub> emissions from fossil fuel combustion and cement production ~~of-in~~ China ~~was-were~~ 9.9 Gt CO<sub>2</sub> in 2016, accounting for ~~about approximately~~ 28% of all global fossil-fuel based CO<sub>2</sub> emissions (Le Quéré et al., 2018; IPCC AR5, 2013). To avoid the potential adverse effects from climate change (Zeng et al., 2008; Qin et al., 2016), the Chinese government has pledged to peak its CO<sub>2</sub> emissions by 2030 or earlier and to reduce ~~the~~CO<sub>2</sub> emissions per unit gross domestic product (GDP) by 60-65% ~~below-less than the~~ 2005 levels (SCIO, 2015). Thus, an accurate quantification of China's CO<sub>2</sub> emissions is the first step ~~in-toward~~ understanding its carbon budget and making carbon control policy.

~~Chinese-The~~ total emission estimates for China are thought to be uncertain or biased due to the lack of reliable statistical data and/or the use of generic emission factors (EF) (e.g., (Guan et al., 2012); (Liu et al., 2015b)). National and provincial data-based inventories used activity data from different sources. The Carbon Dioxide Information Analysis Center (CDIAC) uses ~~and~~ national energy statistics from ~~the~~ United Nations (UN) (Andres et al., 2012), and both the Open-Data Inventory for Anthropogenic Carbon Dioxide (ODIAC) and Global Carbon Project (GCP) mainly use CDIAC total estimates, and thus, they are identical in time series (Le Quéré et al., 2018; Oda et al., 2018). The Emissions Database for Global Atmospheric Research (EDGAR) and Peking University CO<sub>2</sub> (PKU-CO<sub>2</sub>, hereafter named ~~as~~PKU) derived emissions from the energy balance statistics of the International Energy Agency (IEA) (Janssens-Maenhout et al., 2019a; Wang et al., 2013). ~~On-the other hand~~In contrast, ~~the~~ provincial data-based inventories developed within China all used ~~the~~ provincial energy balance sheet ~~in-from the~~ China Energy Statistics Yearbook (CESY), ~~from~~ National Bureau of Statistics of China (NBS) (Cai et al., 2018; Liu et al., 2015a; Liu et al., 2013; Shan et al., 2018). ~~As-for EF, th~~There are generally four sources of EF, i.e., 1) The Intergovernmental Panel on Climate Change (IPCC) default values, which that has-have been adopted by ODIAC and EDGAR (Andres et al., 2012; Janssens-Maenhout et al., 2019b; Oda et al., 2018); 2) National Development and Reform

70 Commission (NDRC) (NDRC, 2012b); 3) China's National Communication, which reported to the United Nations Framework Convention on Climate Change (UNFCCC) (NDRC, 2012a); and 4) The China Emission Accounts and Datasets (CEADs) EF, ~~which that~~ are locally optimized through large sample measurements (Liu et al., 2015b). The existing estimates of global total FFCO<sub>2</sub> emissions are comparable in magnitude, with an uncertainty ~~that is~~ generally within ±10% (Le Quéré et al., 2018; Oda et al., 2018). However, there are ~~great-significant~~ differences ~~in these values~~ at ~~the~~ national scale (Marland et al., 2010; Olivier et al., 2014), with the uncertainty ranging from a few percent to more than 50% in ~~the~~ estimated emissions for individual countries (Andres et al., 2012; Boden et al., 2016; Oda et al., 2018).

Along with ~~the~~ total emissions estimates, ~~the~~ spatial distribution of emissions ~~are-is also~~ important for several reasons: 1) Spatial gridded products ~~provide-enhance our~~ basic understandings ~~on-of~~ CO<sub>2</sub> emissions; 2) ~~They-Spatial distributions~~ are key inputs (as priors) for transport and data assimilation models, ~~and-which~~ influenced the carbon budget (Bao et al., 2020); 80 ~~and 3) For high-emissions areas recognized by multiple inventories, they spatial distributions~~ can be used for policy making ~~in-toward~~ emissions reductions and can provide useful information for ~~the~~ deployment of instruments in emissions monitoring ~~for high-emissions areas recognized by multiple inventories~~ (Han et al., 2020). At the global level, gridded emissions datasets are often based on ~~the~~ disaggregation of country-scale emissions (Janssens-Maenhout et al., 2017; Wang et al., 2013). Thus, ~~the~~ gridded emissions ~~data~~ are subjected to errors and uncertainties ~~from-due to the~~ total emissions 85 ~~calculations~~ and emissions spatial disaggregation (Andres et al., 2016; Oda et al., 2018; Oda and Maksyutov, 2011). For example, the Carbon Dioxide Information Analysis Center (CDIAC) distributes national energy statistics at a resolution of 1°×1° using ~~the~~ population density as a proxy (Andres et al., 2016; Andres et al., 2011). Further, to improve ~~the~~ spatial resolution of ~~the~~ emissions inventory, the Open-Data Inventory for Anthropogenic Carbon dioxide (ODIAC) distributes national emissions based on CDIAC and BP statistics with satellite nighttime lights and power plant emissions (Oda et al., 90 2018; Oda and Maksyutov, 2011). ~~(EDGAR)-derives~~ emissions from the energy balance statistics of the International Energy Agency (IEA); and ~~obtains~~ country-specific activity datasets from BP plc, United States Geological Survey (USGS), World Steel Association, Global Gas Flaring Reduction Partnership (GGFR)/U.S. National Oceanic and Atmospheric Administration (NOAA) and International Fertilizer Association (IFA). Gridded emissions maps at ~~a resolution of 0.1°×0.1°~~ ~~were-are~~ produced using spatial proxy data based on ~~the~~ population density, traffic networks, nighttime lights and point 95 sources, as described in Janssens-Maenhout et al. (2017). Based on ~~the sub-subnational fuel-data~~, population and other geographically resolved data, a high-resolution inventory of global CO<sub>2</sub> emissions was developed at Peking University (Wang et al., 2013).

~~In order to~~To accurately calculate emissions, a series of efforts have been conducted to quantitatively evaluate China's CO<sub>2</sub> emissions using national or provincial activity data, local EF<sub>7</sub>, and detailed data-sets of point sources (Cai et al., 2018; Li et al., 100 2017; Wang et al., 2013). The China High Resolution Emission Database (CHRED) was developed by Cai et al. (2018) and

Wang et al. (2014) based on ~~the~~ provincial statistics, traffic network, point sources and industrial and fuel-specific EF. CHRED was featured ~~by~~ based on its exclusive point source data ~~for~~ from 1.58 million industrial enterprises from the First China Pollution Source Census. The ~~Multi~~ Multi-resolution Emission Inventory for China (MEIC) was developed by Zhang et al. (2007), Lei et al. (2011) and Liu et al. (2015a) at Tsinghua University through ~~integrating~~ the integration of provincial statistics, unit-based power plant emissions, population density, traffic networks, and ~~emission factor (EF)~~ EF (Li et al., 2017; Zheng et al., 2018b; Zheng et al., 2018a). The MEIC uses ~~the~~ China Power Emissions Database (CPED), ~~and in which~~ the unit-based approach is used to calculate emissions for each coal-fired power plant in China with detailed unit-level information (e.g., coal use, geographical coordinates). ~~For~~ Regarding mobile emissions sources, a high-resolution mapping approach is adopted to constrain ~~the~~ vehicle emissions using a county-level activity database. CEADs was constructed by (Shan et al., 2018; Shan et al., 2016) and Guan et al. (2018) based on different levels of inventories to provide emissions at the national and provincial scales. CEADs used coal EF from ~~the~~ large-sample measurements (602 coal samples and samples from 4,243 coal mines). ~~And this is~~, which are assumed to be more accurate than the IPCC default EFs.

However, ~~Regardless of these efforts~~, ~~however~~, ~~the amount of~~ China's CO<sub>2</sub> emissions remains uncertain due to the large discrepancy among current estimates, of which the difference ranges from 8-24% of ~~the~~ total estimates (Shan et al., 2018; Shan et al., 2016). Several studies ~~have made~~ undertaken efforts ~~of quantifying to quantify~~ the possible uncertainty in China's FFCO<sub>2</sub>, such as differences ~~from~~ due to estimation approaches (Berezin et al., 2013), energy statistics (Hong et al., 2017; Han et al., 2020), spatial scales (Wang and Cai, 2017), and point source data. Importantly, the authors ~~would like to point out~~ note that the lack of a comprehensive understanding and comparison of the potential uncertainty in estimates of China's FFCO<sub>2</sub>, including spatial, temporal, proxy, and magnitude components, ~~makes~~ causes Chinese emissions ~~possible data to be~~ more uncertain, and thus, it is important to present, analyze and explain such differences among inventories.

Here, we evaluated the uncertainty in China's FFCO<sub>2</sub> estimates by synthesizing global gridded emissions datasets (ODIAC, EDGAR, and PKU) and China-specific emission maps (CHRED, MEIC, and the Nanjing University CO<sub>2</sub> (NJU) emission inventory). Moreover, several other inventories were used in the evaluation analysis, such as the Global Carbon Budget from the Global Carbon Project, ~~and~~ and the National Communication on Climate Change of China (NCCC).

The ~~purposes~~ aims of this study were to: 1) ~~Quantify~~ the magnitude and the uncertainty in China's FFCO<sub>2</sub> estimates using the spread of values from ~~the~~ state-of-the-art inventories; 2) identify the spatiotemporal differences of China's FFCO<sub>2</sub> emissions ~~between~~ among the existing emission inventories and explore the underlying reasons for such differences. To our knowledge, this is the first comprehensive evaluation of the most up-to-date and ~~mostly~~ predominantly publicly available carbon emission inventories for China.

## 2. Emissions data

The ~~An~~ evaluation analysis was conducted from ~~9 inventories including six~~ 6 gridded datasets (listed in Table 1, ~~ODIAC, EDGAR, PKU, CHRED, MEIC, and NJU~~) and ~~three~~ 3 other ~~datasets (GCP/CDIAC, CEADs, and NCCC)~~ containing statistical data. We selected ~~the~~ year 2012 for spatial analysis ~~since because~~ this is the most recent year available for all ~~the~~ gridded data-sets and also ~~because this is~~ 2012 was a peak year of emissions due to the strong reductions ~~from following the~~ impacts of the 12th-Five-Year-Plan. Specifically, the global fossil fuel CO<sub>2</sub> emissions datasets included the year 2017 version of ODIAC (ODIAC2017), ~~the~~ version ~~v~~4.3.2 of EDGAR (EDGARv4.3.2) ~~and~~, PKU-CO<sub>2</sub>, ~~all of~~ which ~~all~~ used the Carbon Monitoring for Action (CARMA) as ~~the~~ point source. The China-specific emissions data used were ~~the dated from the~~ ~~year from~~ 2007 ~~of from~~ CHRED, ~~the~~ MEIC v1.3 ~~and~~, NJU-CO<sub>2</sub> v2017, ~~all of~~ which ~~all~~ used China Energy Statistical Yearbook (CESY) activity data. Moreover, ~~three~~ 3 inventories were used as ~~a~~ references, i.e., GCP/CDIAC, CEADs and NCCC, ~~since because~~ GCP and ODIAC used CDIAC for ~~most the majority~~ of the years, except ~~for~~ the ~~most~~-recent two years, ~~that which~~ were extrapolated ~~by using~~ BP data. ~~These three inventories~~ were treated as ~~inventory one~~ in a time series comparison. Data were collected from ~~the~~ official websites ~~for of~~ ODIAC, EDGAR, PKU, and ~~6 six~~ tabular statistical ~~al~~ data ~~sets~~, and were ~~also~~ acquired from ~~their the~~ authors ~~for of who developed~~ CHRED, MEIC and NJU. See ~~the~~ supporting information for more details ~~on of the~~ data sources and ~~the~~ methodology ~~of used for~~ each dataset.

## 3. Methodology for ~~the~~ evaluation of multiple datasets

We evaluated ~~these the abovementioned~~ datasets from three aspects: data sources, boundary (emission sectors) and methodology (Figure 1, Table 1 and S1, S2). ~~For In regard to the~~ data source, there are two levels: national data, such as UN or IEA statistics, and provincial-level data, such as CESY. The emission sectors mainly include fossil fuel production, industry production and processes, households, transportation, aviation/shipping, agriculture, natural biomass burning from wild fires and ~~the~~ waste ~~for from~~ these datasets, ~~and where~~; Table S1 lists ~~the ed~~ sectors included in each inventory. ~~And In addition~~, for methodology, ~~the~~ analysis of ~~the~~ inventories includes ~~the~~ total estimates (activity data and EF) aspect and ~~the~~ spatial disaggregation of point, line and area sources. ~~As Fig. 1 depicts shows depicted~~ the conceptual procedure ~~followed in~~ ~~for the~~ total emissions estimates and how ~~the~~ gridded maps ~~are were~~ produced for all ~~the~~ inventories, ~~and thus~~, it is important to know the differences in ~~the~~ activity data, EF and spatial proxy data and spatial disaggregation methods ~~they~~ used ~~by~~ ~~previous scholars~~, to understand the differences among ~~the~~ inventories in ~~regard to~~ total emissions estimates and spatial characteristics.

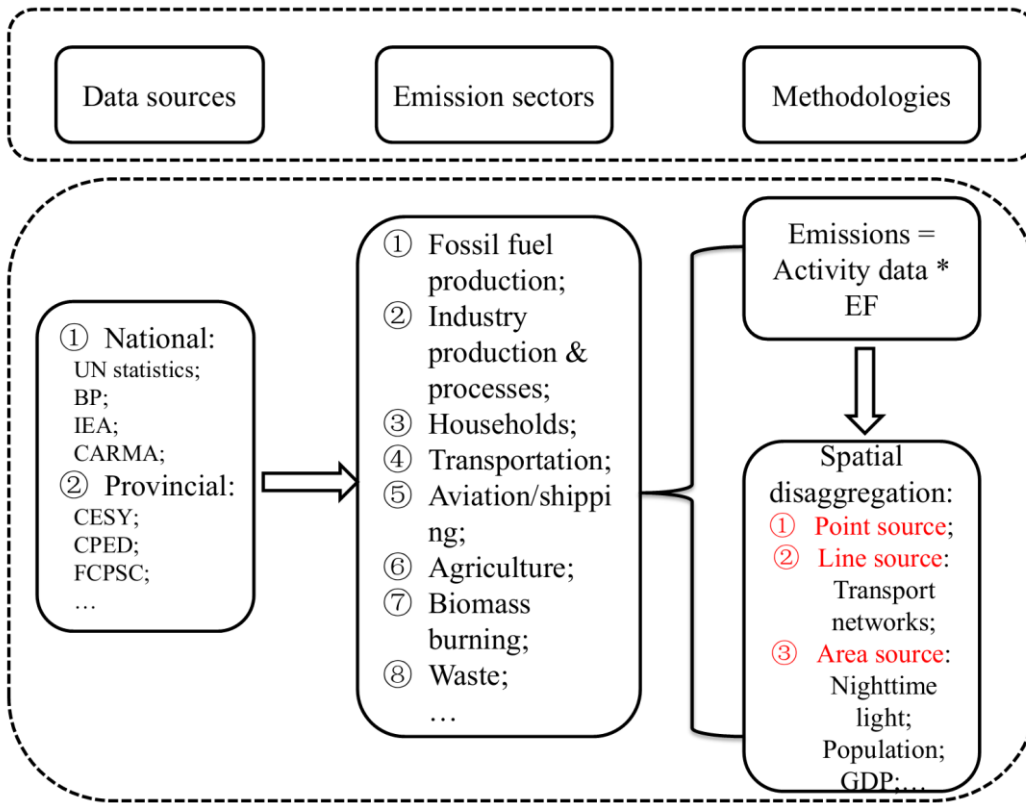


Figure 1 Conceptual diagram for data evaluation based on data sources, emission sectors and methodologies.

160 ~~Preprocessing~~ The preprocessing of six gridded CO<sub>2</sub> emission datasets included several steps, which that are described as follows. First, ~~the~~ global maps of CO<sub>2</sub> emissions (i.e., ODIAC, EDGAR and PKU) were re-projected ~~to using the~~ Albers Conical Equal Area projection (that of CHRED). ~~And Next,~~ the nearest neighbor algorithm was used to resample different spatial resolutions s into a pixel size of 10 km ~~x by~~ 10 km, and this method takes the value from the cell closest to the transformed cell as the new value. Second, the national total emissions were derived using the ArcGIS zonal statistics tool

165 ~~for from~~ CHRED, while the ~~other others~~ emissions were from tabular data provided by the data owners. Finally, the grids for each inventory were sorted in ascending order and then plotted on a logarithmic scale to represent the distribution of emissions. To identify the contribution of high emission grids, emissions at the grid level that exceeded 50 kt CO<sub>2</sub> yr<sup>-1</sup> km<sup>-2</sup> and the top 5% emitting grids were selected for analysis.

Table 1 General information ~~for~~ of the emissions data-sets\*

| Data  | ODIAC2017         | EDGARv432         | PKU               | CHRED                     | MEIC                  | NJU                   | CEADs                 | GCP/CDIAC         | NCCC             |
|---|-------------------|-------------------|-------------------|---------------------------|-----------------------|-----------------------|-----------------------|-------------------|------------------|
| Domain  | Global            | Global            | Global            | China                     | China                 | China                 | China                 | Global            | China            |
| Temporal coverage                               | 2000-2016         | 1970-2012         | 1960-2014         | 2007, 2012                | 2000-2016             | 2000-2015             | 1997-2015             | 1959-2018         | 2005, 2012, 2014 |
| Temporal resolution                             | Monthly           | Annual            | Monthly           | Biennially or triennially | Monthly               | Annual                | Annual                | Annual            | Annual           |
| Spatial resolution                              | 1 km              | 0.1 degree        | 0.1 degree        | 10 km                     | 0.25 degree           | 0.25 degree           | N/A                   | N/A               | N/A              |
| Emission estimates                              | Global & National | Global & National | Global & National | National & Provincial     | National & Provincial | National & Provincial | National & Provincial | Global & National | National         |
| Emission factor for raw coal (tC per t of coal) | 0.746             | 0.713             | 0.518             | 0.518                     | 0.491                 | 0.518                 | 0.499                 | 0.746             | 0.491            |
| Uncertainty                                     | 17.5% (95% CI)    | ±15%              | ±19% (95% CI)     | ±8%                       | ±15%                  | 7-10% (90% CI)        | -15% - 25% (95% CI)   | 17.5% (95% CI)    | 5.40%            |
| Point   | CARMA             | CARMA3.0          | CARMA2.0          | FCPSC                     | CPED                  | CEC;A                 | N/A                   | N/A               | N/A              |

|                        |                 |  |  |  |                              |                           |       |      |      |
|------------------------|-----------------|--|--|--|------------------------------|---------------------------|-------|------|------|
| source                 | 2.0             |  |  |  |                              | CC;CC<br>TEN              |       |      |      |
| Line source            | N/A             | the OpenStreetMap and OpenRailwayMap, Int. aviation and bunker | N/A  | The national road, railway, navigation network <sub>25</sub> and traffic flows | Transport networks           | N/A                       | N/A   | N/A  | N/A  |
| Area source            | Nighttime light | Population density, nighttime light                            | Vegetation and population density, nighttime light | Population density, land use <sub>25</sub> human activity                      | Population density, land use | Population density, GDP   | N/A   | N/A  | N/A  |
| Version name           | ODIAC2017       | EDGARv4.3.2_FT2016, EDGARv4.3.2                                | PKU-CO2-v2   | CHRED  | MEIC v.1.3                   | NJU-CO <sub>2</sub> v2017 | CEADs | N/A  | N/A  |
| Year published/updated | 2018            | 2017   | 2016   | 2017   | 2018                         | 2017                      | 2017  | 2019 | 2018 |



|              |   |   |   |   |   |                            |   |   |   |
|--------------|---|---|---|---|---|----------------------------|---|---|---|
| Data sources | <a href="http://db.cger.nies.go.jp/dataset/ODI/AC/">http://db.cger.nies.go.jp/dataset/ODI/AC/</a> | <a href="http://edgar.jrc.ec.europa.eu/overview.php?v=432_GHG&amp;SECURE=123">http://edgar.jrc.ec.europa.eu/overview.php?v=432_GHG&amp;SECURE=123</a> | <a href="http://inventory.pku.edu.cn/download/download.html">http://inventory.pku.edu.cn/download/download.html</a> | Data developer  | Data developer                                  | Data developer             | <a href="http://www.ceads.net/(registrationrequired)">http://www.ceads.net/(registrationrequired)</a> | <a href="https://www.globalcarbonproject.org/carbonbudget/19/data.htm">https://www.globalcarbonproject.org/carbonbudget/19/data.htm</a> | <a href="https://unfccc.int/sites/default/files/resource/China2BUR_English.pdf">https://unfccc.int/sites/default/files/resource/China2BUR_English.pdf</a> |
| References   | <a href="#">Oda (2018)</a>  | <a href="#">Janssens-Maenhout (2017)</a>  | <a href="#">Wang et al., 2013</a>   | <a href="#">Cai et al. (2018); Wang et al. (2014)</a> | <a href="#">Zheng (2018); Liu et al. (2015)</a> | <a href="#">Liu (2013)</a> | <a href="#">Shan et al. (2018)</a>  | <a href="#">Friedlingstein et al. (2019)</a>  | <a href="#">NCCC (2018)</a>   |

170 \* CI: Confidence interval; FCPSC: the First China Pollution Source Census; CPED: China Power Emissions Database; CEC: Commission for Environmental Cooperation;

171 ACC: China Cement Almanac; CCTEN: China Cement Industry Enterprise Indirectory; GDP: Gross domestic product; N/A: Not available.

## 4. Results

### 4.1 Total emissions and recent trends

The interannual variations of China's CO<sub>2</sub> emissions from 2000 to 2016 were evaluated from ~~six~~<sup>6</sup> gridded emission maps and ~~three~~<sup>3</sup> national total inventories (Figure 2). All ~~the~~ datasets show a significant increasing trend in the period of 2000 to 2013 from 3.4 to 9.9 Gt CO<sub>2</sub>. The range of the ~~nine~~<sup>9</sup> estimates increased simultaneously from 0.7 to 2.1 Gt CO<sub>2</sub> (both are 21% of the corresponding years' total emissions). In the second period (from 2013 to 2016), the temporal variations mostly levelled off or even decreased. Specifically, the emissions estimated from PKU and CEADs showed a slight downward trend, ~~even though although~~ they used independent activity data ~~of from~~ IEA (2014) and National Bureau of Statistics (2016), and this downward trend ~~is was~~ attributed to changes in ~~the~~ industrial structure, improved combustion efficiency, emissions control and slowing economic growth (Guan et al., 2018;Zheng et al., 2018a).

There is a large discrepancy among the current estimates, ranging from 8.0 to 10.7 Gt CO<sub>2</sub> in 2012. NJU ~~has had~~ the highest emissions during the periods of 2005—2015, followed by EDGAR, MEIC and CDIAC/GCP/ODIAC, while CEADs (National) and PKU were ~~much significantly~~ lower (Figure 2). ~~This~~ ~~These discrepancies are~~ ~~is~~ mainly because of three reasons: 1) the EF for raw coal was ~~higher greater~~ for EDGAR and ODIAC than the other ~~databases~~. The EFs were different for different fossil fuel types and cement production (Table S2). ~~Since~~ ~~Because~~ coal consumption ~~consisted constituted~~ 70-80% of total emissions, ~~the~~ coal EF ~~is was~~ more significant than the others. The EFs were different for ~~the~~ three major fossil fuel types (raw coal, oil and natural gas) and cement production (Table 1 and S2). ~~And~~ ~~In addition, they the EFs are were~~ ~~obtained~~ from either ~~the~~ IPCC default values or local optimized values from different sources. ~~They~~ ~~The EFs~~ do not change over time in these inventories, although they should, due to the unavailability of EFs over time; 2) differences in activity data, ~~i.e.,~~ NJU, MEIC and CEADs (Provincial) used ~~d~~ provincial data from CESY (2016), while CEADs (National) ~~and~~; PKU used ~~d~~ national data from CESY (2016) and IEA (2014), respectively (Table 1 and S1), ~~and such that the~~ sum of provincial emissions ~~would be~~ higher than the national total; ~~and~~ 3) differences in emission definitions (Table 1 and S1, emissions sectors). Although we tried to ~~make ensure that~~ these datasets ~~would be~~ as comparable as possible, ~~there are still nonetheless~~ minor differences in emissions sources (sectors) ~~remained~~. For example, EDGAR contains abundant industry process-~~related~~ emissions, ~~while whereas~~ CEADs only consider~~ed~~ cement production (Janssens-Maenhout et al., 2019b). EDGAR and MEIC have ~~a~~ similar trends, ~~but except for their~~ magnitudes, ~~whereand~~ MEIC is usually ~~higher greater~~ than EDGAR. This is a combined effect of the above three reasons. ~~Moreover,~~ MEIC uses ~~the~~ provincial energy data ~~from~~ CESY (2016), ~~while whereas~~ EDGAR uses~~d~~ ~~the~~ national-level data ~~from~~ IEA (2014). ~~But~~ ~~However,~~ MEIC's EF is lower than ~~that of~~ EDGAR. These opposing effects ~~would~~ bring ~~them the data sets~~ closer in magnitude. ~~The~~ ~~Both the~~ gridded

products (ODIAC, EDGAR, MEIC and NJU) and national inventory (GCP/CDIAC) both show small differences in the magnitude of total emissions estimates and trends from 2000—2007, and where the differences in magnitude increase gradually from 2008 onward. Although the range increases with time, the relative difference remains at around approximately 21% of the corresponding years' total estimates, indicating potentially systematic differences, such as the fact that EFs remain stable.

205

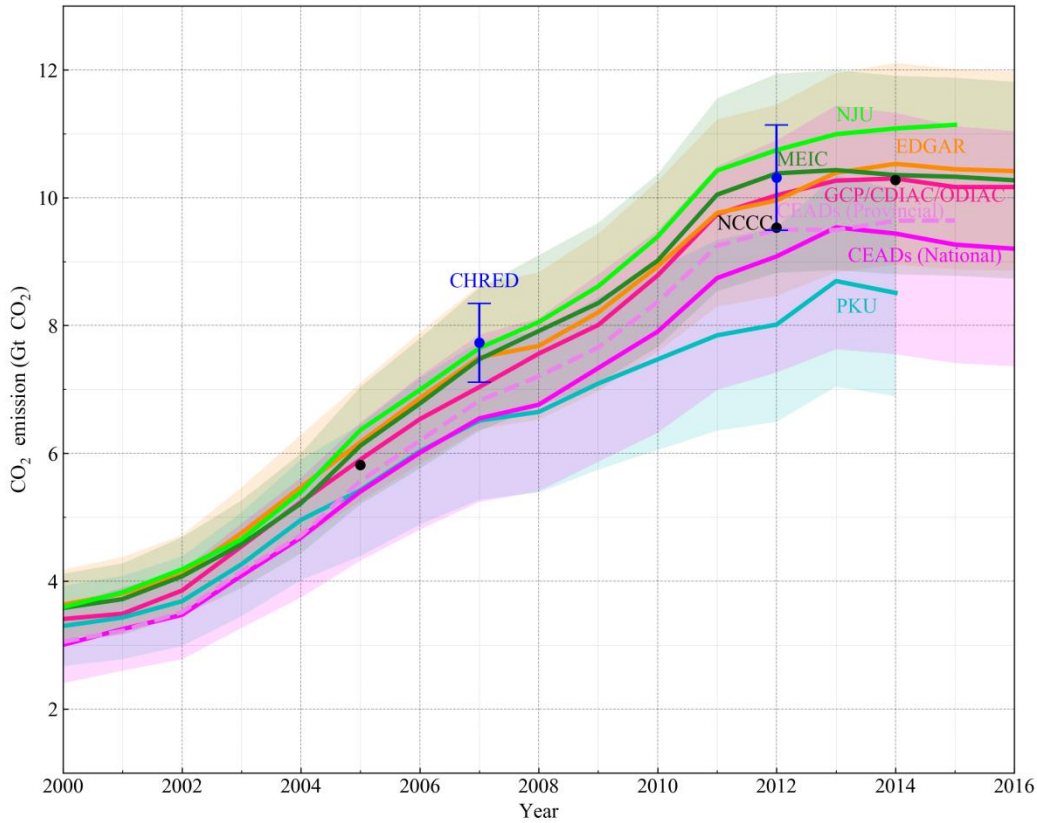


**Figure 2.** China's total FFCO<sub>2</sub> emissions from 2000 to 2016. The emissions are from the combustion of fossil fuels and cement production from different sources (EDGARv4.3.2\_FT2016 includes international aviation and marine bunkers emissions). To keep—maintain comparability and avoid differences resulting from the emissions disaggregation— (e.g., Oda et al. 2018(Oda et al., 2018)), the values for of the six gridded emission inventories are tabular data provided by the data developers before spatial disaggregation. Prior to 2014, GCP data was—were taken from CDIAC, and those from 2015–2016 was—were calculated based on BP data and the fraction of cement production emissions in 2014. The shaded area (error bar for CHRED) indicates uncertainties from the coauthors' previous studies (See Table 1).

210

#### 4.2 Spatial distribution of FFCO<sub>2</sub> emissions

The evaluation of spatially—explicit FFCO<sub>2</sub> emissions is fundamentally limited by the lack of direct physical measurements on—at the grid scales (e.g., (Oda et al., 2018)). We thus—Thus, we attempted to characterize the spatial patterns of China's carbon emissions by presenting the available emissions estimates—available. We compared six gridded products, including ODIAC, EDGAR, PKU, CHRED, MEIC and NJU, in—for the year 2012.—The, which —year 2012—was the most recent year for which all the six datasets were available. Spatially, the CO<sub>2</sub> emissions from the different datasets are concentrated in eastern China (Figure 3). High—The high—emission areas were mostly distributed in city clusters (e.g., BeijingTianjin-Hebei

220

(Jing-Jin-Ji), the Yangtze River Delta, and the Pearl River Delta) and densely populated areas (e.g., the North China Plain, the Northeast China Plain and Sichuan Basin). These major spatial patterns are primarily due to the use of spatial proxy data, and ~~also are~~ are also in accordance with previous studies (Guan et al., 2018; Shan et al., 2018). However, there were notable differences among the different estimates at finer spatial scales. ~~The~~ Large carbon emissions regions were found in the North China Plain and the Northeast China Plain for ODIAC (Figure 3a), PKU (Figure 3c), MEIC (Figure 3e) and NJU (Figure 3f), which ranged from 1000 to 10,000 t CO<sub>2</sub>/km<sup>2</sup>. However, ~~the~~ high levels of emissions located in the Sichuan Basin were found from PKU, MEIC and NJU, but not from ODIAC. This discrepancy in identifying ~~the large significant~~ CO<sub>2</sub> emissions was probably due to ~~the~~ emissions from rural settlements with high population densities (e.g., Sichuan Basin), which did not appear strongly in satellite nighttime lights ~~and or on the~~ ODIAC map (Wang et al., 2013). The more diffusive distributions ~~for of~~ MEIC and NJU ~~is were~~ attributed to the abundance of point sources ~~abundance~~, with or without line sources and area sources proxies. ~~Besides, Moreover,~~ EDGAR, PKU, CHRED, MEIC and NJU all showed relatively low emissions in western China, but the emissions from ODIAC ~~was were~~ zero due to ~~no the lack of~~ nighttime light ~~therein that~~ region, which tended to distribute more emissions towards ~~strongly nightlights lit (at night)~~ urban regions (Wang et al., 2013).

EDGAR, CHRED and MEIC all showed ~~the~~ traffic line source emissions by inducing traffic networks in the spatial disaggregation. The line emissions (such as expressways, arterial highways) depicted a more detailed spatial distribution in CHRED than in either EDGAR ~~and or~~ MEIC. This discrepancy could be attributed to the different road networks and corresponding weighting factors ~~they that were~~ used by each. CHRED disaggregated emissions from the transport sector based on traffic networks and traffic flows (Cai et al., 2018). MEIC applied the traffic network from the China Digital Road-network Map (CDRM) (Zheng et al., 2017), and EDGAR traffic networks were obtained from the OpenStreetMap and OpenRailwayMap (Geofabrik, 2015). ODIAC considered point and area sources ~~and was lack~~ while lacking of line source emissions in the spatial disaggregation, which ~~would put places~~ more emissions ~~towards in~~ populated areas than in suburbs (Oda et al., 2018). Oda and Maksyutov (2011) (Oda and Maksyutov, 2011) ~~pointed out~~ noted the possible utility of ~~the~~ street lights to represent line source spatial distributions even without the associated specific traffic spatial data. The spatial distributions of traffic emissions are highly uncertain, with biases of 100% or more (Gately et al., 2015), which is largely due ~~largely~~ to mismatches between the downscaling proxies and the actual vehicle activity distribution.

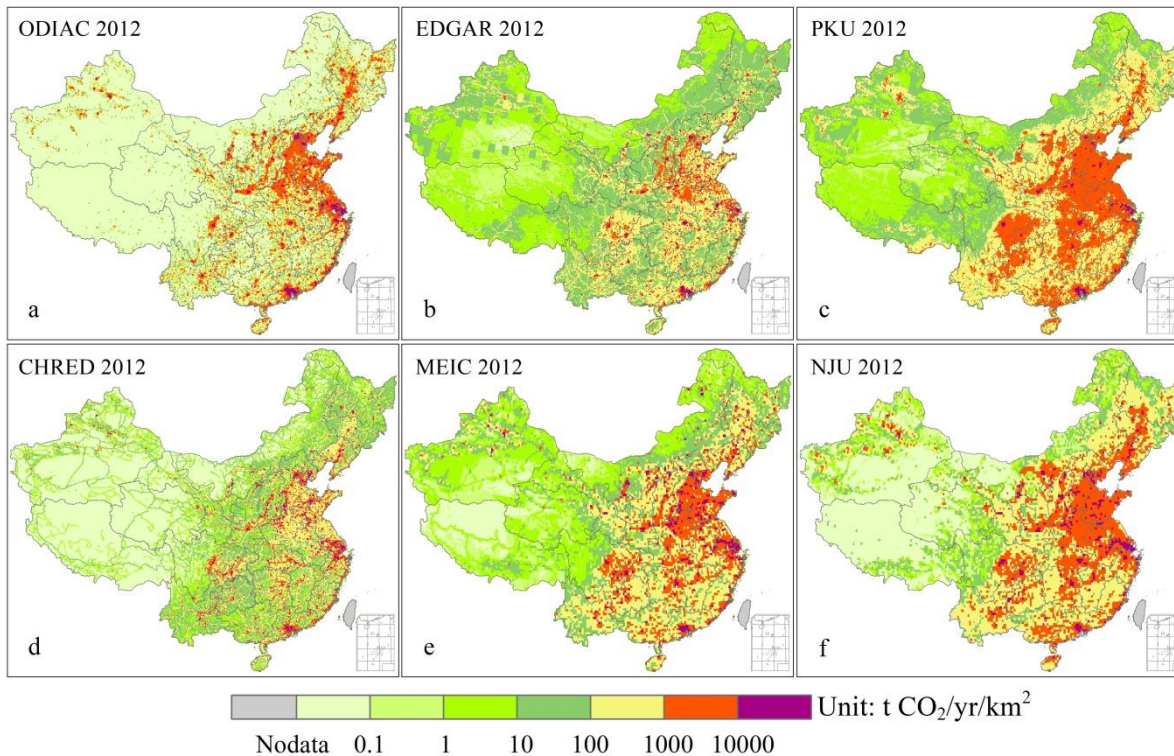


**Figure 3.** Spatial distributions of ODIAC (a), EDGAR (b), PKU (c), CHRED (d), MEIC (e) and NJU (f) at a 10 km resolution for 2012. ODIAC was aggregated from 1 km data, such that MEIC, PKU, and EDGAR was/were resampled from 0.25, 0.1 and 0.1 degrees.

250

#### 4.3 CO<sub>2</sub> emissions at the provincial level

The provincial level results showed more consistency than the grid level results in terms of spatial distribution. All the products agreed that the eastern and southern provinces are/were high emitters (>400 Mt CO<sub>2</sub>/yr, Figure 4 and S3), and while the western provinces were low emitters (<200 Mt CO<sub>2</sub>/yr, Figure 4 and S3). The top-five greatestmost emitting provinces were Shandong, Jiangsu, Hebei, Henan, and Inner Mongolia, with the amount the emissions values ranging from 577 ± 48 Mt to 820 ± 102 Mt CO<sub>2</sub> in 2012 (Figure 4). While-Meanwhile, the provinces located in the western area with low economic activity and population density showed low carbon emissions (<200 Mt CO<sub>2</sub>, Figure 4 and S3). There is a clear discrepancy in the provincial-level emissions among the different estimates, and the mean standard deviation (SD) for the 31 provinces' emissions was 62 Mt CO<sub>2</sub> (or 20%) in 2012. A large SD (>100 Mt CO<sub>2</sub>) occurred in the high-emitting provinces, such as Shandong, Jiangsu, Inner Mongolia, Shanxi, Hebei, and Liaoning. For the Shandong provinceProvince, the inventories varied from 675-965 Mt CO<sub>2</sub>/yr, with a relative SD of 12% (Figure 4 and 5), and for the other high-emitting provinces, the relative SD ranged from 12%--48%, which. This implied that there is still room to reduce the uncertainty could be further

260

reduced.

265 ~~Since~~ ~~Because~~ estimates based on provincial energy statistics are assumed to be more accurate than those derived from ~~the~~ disaggregation of national totals using spatial proxies, we evaluated the provincial emissions of each inventory using the provincial-based inventory mean (CHRED, MEIC, and NJU) (Figure 5). The results showed that emissions derived from the provincial energy statistics are highly correlated, with R-values ranging from 0.99 to 1.00 and slopes ranging 0.96 to 1.04. ~~By~~ ~~In~~ contrast, the estimates for ODIAC, EDGAR, and PKU, which used IEA national energy statistics, showed an obvious disparity, especially in the ~~top 5 five greatestmost~~ -emitting provinces, suggesting the ~~large-significant~~ impact of spatial disaggregated approaches in ~~allocating the allocation of~~ total emissions. The potential implication is ~~that~~ when ~~doing~~ ~~performing~~ spatial disaggregation, national-data-based inventories can use provincial fractions as constraints.

270

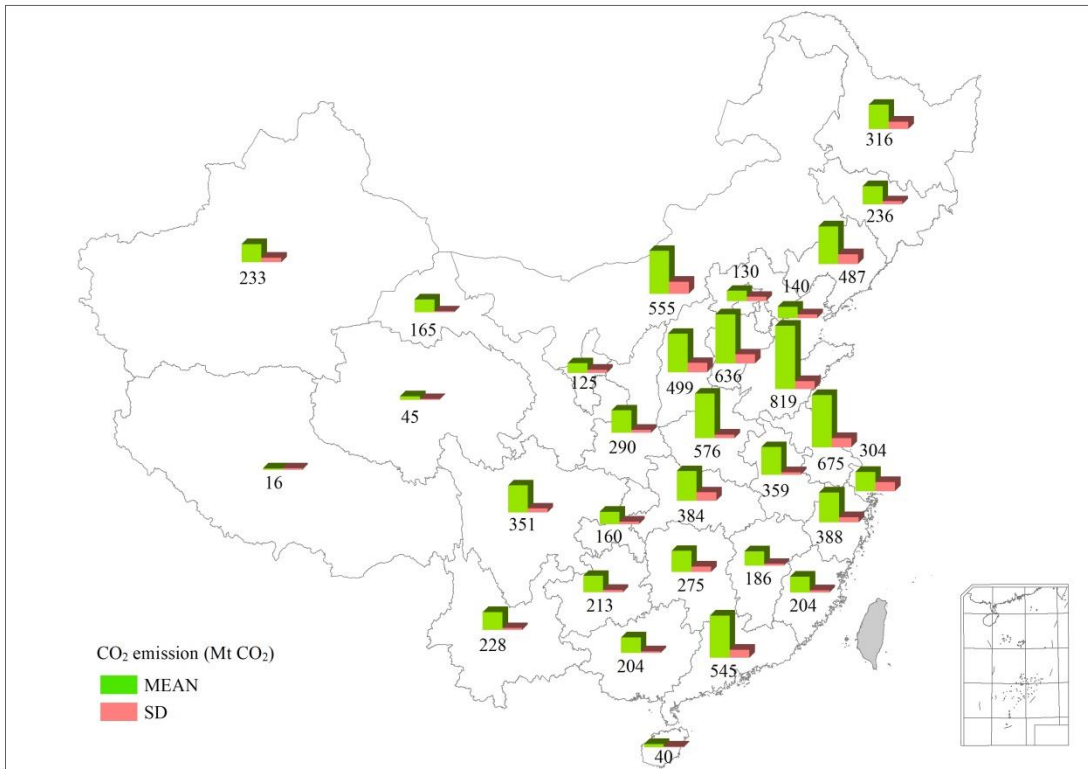
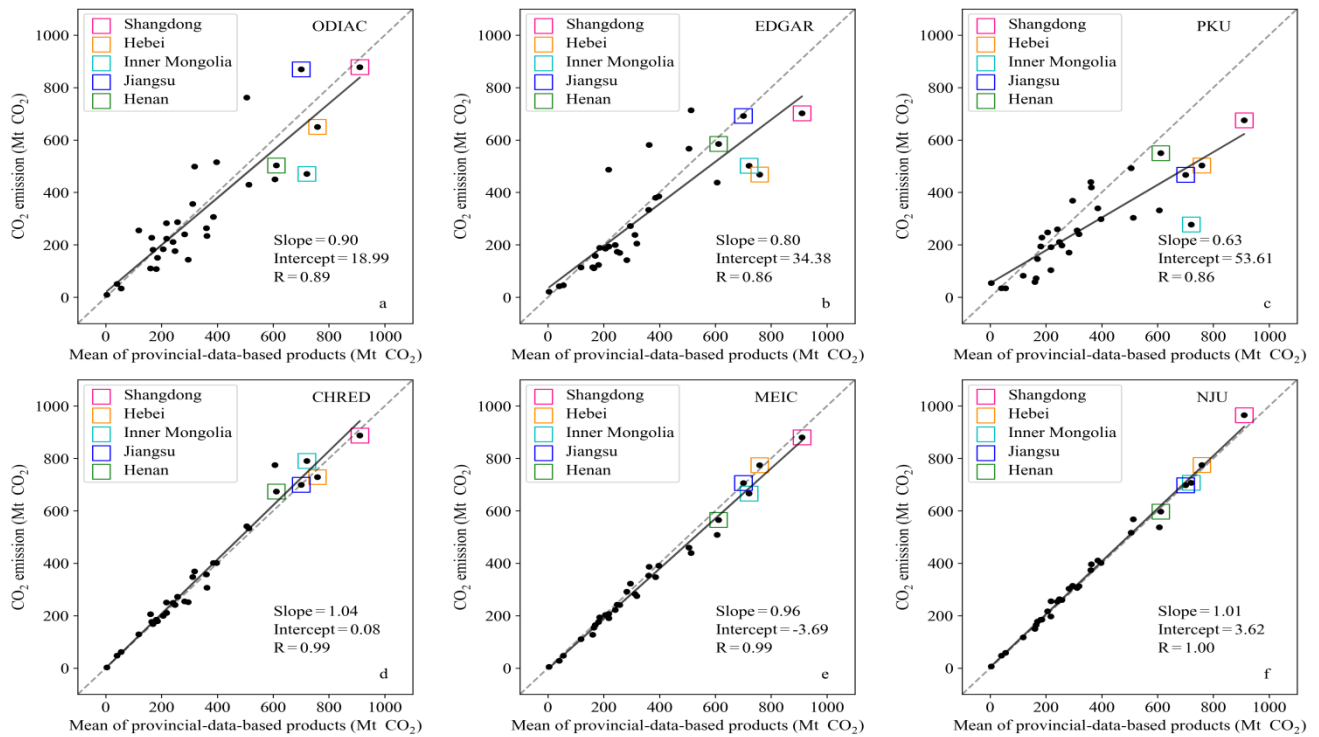


**Figure 4.** Provincial mean total emissions for ODIAC, EDGAR, PKU, CHRED, MEIC and NJU in 2012. ~~The n~~Numbers ~~refer to~~~~beneath~~ the green bars are ~~the~~ provincial total CO<sub>2</sub> emissions in Mt.



275

**Figure 5.** Scatter plots of the provincial total emissions for ODIAC, EDGAR, PKU, CHRED, MEIC and NJU in 2012 with the top 5 five greatest- most emitting provinces highlighted, and the x-axis is the mean of provincial-data-based products (CHRED, MEIC and NJU).

#### 4.4 Statistics of CO<sub>2</sub> emissions at the grid level

To further characterize the spatial pattern of China's CO<sub>2</sub> emissions, the probability density function (PDF), cumulative emissions, and top 5% emitting grids were analyzed to identify the spatial differences from the distribution of grid cell emissions (Figure 6). As illustrated in Figure 4a, ODIAC showed a large-significant number of cells with zero emissions (62%) (Figure 6a), with medium-emitting grids (500-50,000 t CO<sub>2</sub>/km<sup>2</sup>) consisted-constituted 30%, while-and high-emitting grids (>50,000 t CO<sub>2</sub>/km<sup>2</sup>) consisted-constituted 3%. While-Although the low-emissions cells (1-500 t CO<sub>2</sub>/km<sup>2</sup>) were mainly located in EDGAR (58%) and CHRED (69%) (Figure 6b and d), and the medium-emitting grids consisted-constituted 30-40%, while-nonetheless-the high-emitting grids consisted-only amounted to 2-3%. This situation could have a notable-significant impact on the cumulative national total emissions (Figure 6g). The frequency distribution of high-emissions grids revealed the-differences in the point source data. MEIC showed the largest number of high-emitting cells (500-500,000 t CO<sub>2</sub>/km<sup>2</sup>, 5% compared-in comparison with the others, which were at 2-3%, Figure 6e) by using a high-resolution emissions database (CPED) including-that included more power plant information (Li et al., 2017; Liu et al., 2015a). Furthermore, ODIAC and EDGAR showed-a good agreement-agreed well regarding the in-high emissions (>100,000 t CO<sub>2</sub>/km<sup>2</sup>), because because their point source emissions, were both from the CARMA database (Table 1). Moreover,

290

CARMA is the only global database ~~for tracking that tracks~~ CO<sub>2</sub> that gathered and presented the best available estimates of CO<sub>2</sub> emissions for 50,000 power plants around the world, of which ~~around approximately~~ 15,000 have latitude and longitude information with emissions ~~larger greater~~ than 0. The database ~~is responsible for~~ includes approximately about 295 one-quarter of all greenhouse gas emissions. However, CARMA is no longer active (the last update was November 28, 2012), and the geolocations of power plants are not ~~sufficiently accurate enough~~, especially in China (Byers et al., 2019; Liu et al., 2013; Wang et al., 2013; Liu et al., 2015a). Therefore, users ~~have to must perform de~~ corrections themselves (Liu et al., 2013; Oda et al., 2018; Wang et al., 2013; Janssens-Maenhout et al., 2019b; Liu et al., 2015a).

As ~~depicted shown in by~~ the cumulative emissions plot (Figure 6g), PKU and NJU showed very similar cumulative curves, 300 ~~and so and the situation was similarly for did~~ EDGAR and CHRED. Moreover, the total emissions for EDGAR and CHRED were largely determined by a small proportion of high-emitting grids ~~with that showed~~ a steep increase at the last stage of ~~the~~ cumulative curves (Figure 6g), and the top 5% emitting grids accounted for ~~approximately ~~~90% of the total emissions (Figure 6e), ~~higher than those of which is greater than the comparable values of~~ 82%, 71%, 58% and 51% ~~in for~~ ODIAC, MEIC, NJU and PKU, respectively. The emissions from PKU, MEIC and NJU were relatively evenly distributed. ~~This was~~ 305 ~~due to the fact that because~~ CHRED was mainly derived from enterprise-level point sources (Cai et al., 2018). In contrast, the emissions of PKU ~~showed were~~ the most evenly ~~pattern distributed~~, and the emissions from ~~the~~ top 5% emitting grids only accounted for 51% (Figure 6g). ~~This was~~ because PKU ~~had incorporated a~~ special area source survey data for ~~the~~ Chinese rural areas from a 34,489-household energy-mix survey and a 1,670-household fuel-weighting campaign (Tao et al., 2018).

Moreover, the ~~use of a~~ spatial disaggregation proxy ~~using based on~~ population density also contributed to this spatial pattern. 310 Similarly, MEIC and NJU ~~exhibited a even distribution were evenly distributed~~ because of the same activity data from CESY, National Bureau of Statistics (Table 1).



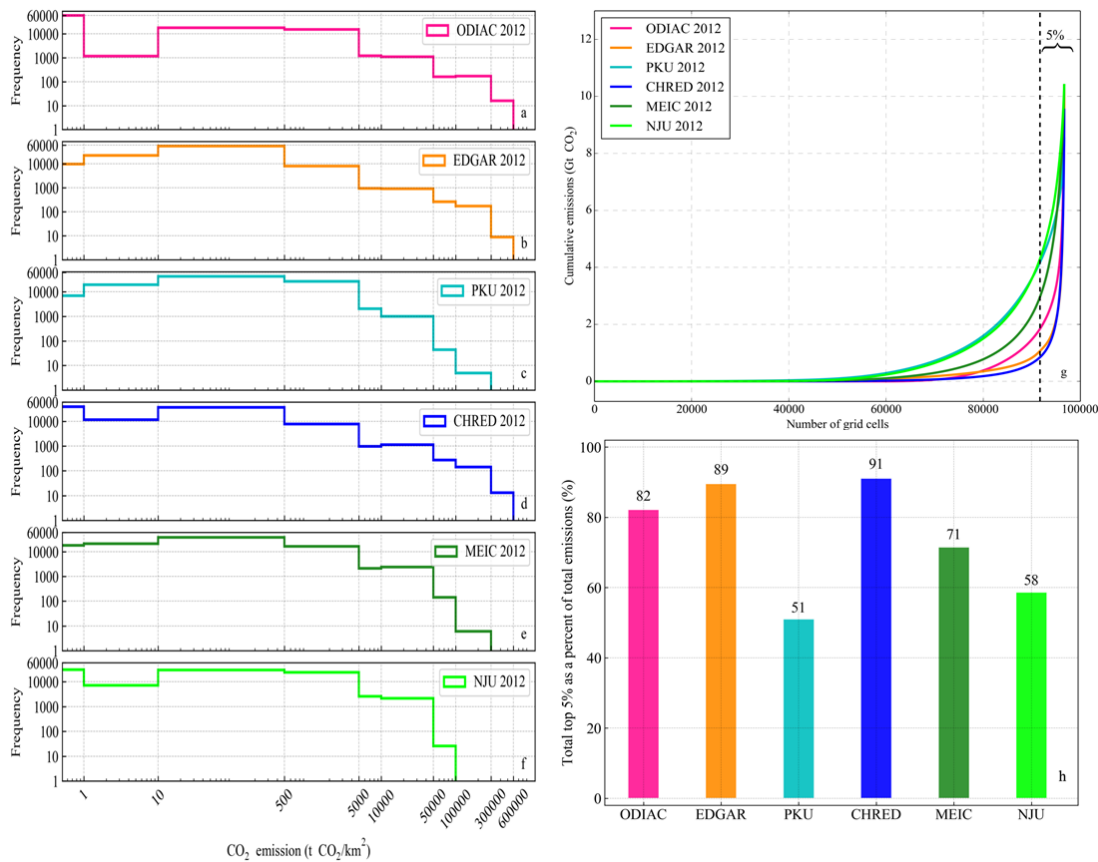


**Figure 6.** Frequency counts (a-f), cumulative emissions (g) (grids were sorted from low to high), and the top 5% emitting grids plots (h) for ODIAC, EDGAR, PKU, CHRED, MEIC and NJU in 2012 at a 10-km resolution.

315 To identify the locations of hotspots, ~~the~~ bubble plots (Figure S2) demonstrated the spatial distribution of high-emitting grid cells that were larger ~~greater~~ than 50 kt CO<sub>2</sub>/km<sup>2</sup>. CHRED, EDGAR and ODIAC showed ~~a~~ similar patterns, with high-emitting grids concentrated in city clusters (e.g., Jing-Jin-Ji, the Yangtze River Delta, and the Pearl River Delta) and the eastern coast (Figure S2). EDGAR and ODIAC both derived the ir power plant emissions from CARMA, but ODIAC was likely to put ~~place~~ more emissions than EDGAR over urbanized regions with lights, especially in the North China Plain. The emissions of CPED and CARMA were similar in China, with a minor difference of 2%, but ~~although~~ the numbers of power plants had ~~a large difference~~ varied significantly (2320 vs. 945) (Liu et al., 2015a), which ~~This~~ implied that CARMA tended to allocate similar emissions to fewer plants than CPED.

320

## 5. Discussion

### 5.1 Activity data differences in the datasets and their effects

325 ~~Activity~~ The activity data sources, data level and sectors were ~~are~~ the significant determinants of ~~the~~ total emissions largely. As can be seen ~~As seen~~ in Fig. 1, activity data and EF determine the total emission estimates, and ~~then~~ affect the spatial distributions through ~~by using~~ disaggregation proxies ~~of~~ for point, line and area sources. It has been well-discussed that the

sum of ~~the~~ provincial data is ~~larger-greater~~ than the national total (Guan et al., 2012; Hong et al., 2017; Liu et al., 2015b; Shan et al., 2018; Liu et al., 2013). CEADs (~~p~~Provincial) is 8-18% ~~higher-greater~~ than CEADs (~~n~~National) after year 2008 (Figure 2). ~~And thus~~ Thus, the province-based estimates (e.g., NJU and MEIC) are ~~higher-greater~~ than CEADs (~~n~~National). This ~~difference~~ could be attributed to the differences in national and provincial statistical systems and artificial factors, such as ~~the fact~~ that some ~~of~~ provincial energy balance sheets were adjusted to ~~make-to~~ achieve ~~the-an~~ exact match between supply and consumption (Hong et al., 2017). For example, ~~the~~ provincial statistics ~~has-suffer from~~ data inconsistency and double counting problems (Zhang et al., 2007; Guan et al., 2012). One possible way to improve ~~these statistics is-is~~ to use the provincial consumption fractions to rescale the national total consumptions when distributing emissions to grids. Hong et al. (2017) found that the ratio of the maximum discrepancy to the mean value was 16% due to ~~the use of~~ different versions of national and provincial data in CESY. Ranges of 32-47% of CO<sub>2</sub> emissions from ~~the~~ power sector (mainly coal use) were found among ~~the~~ inventories, while for ~~the~~ transport sector (mainly liquid fuels), the fractions ranged from 7-9%. Apart from such differences, one peak of FFCO<sub>2</sub> emissions was identified by most datasets in 2013, ~~which were which was due~~ largely ~~found to be due~~ to ~~the~~ slowing economic growth (National Bureau of Statistics, 1998–2017), changes in ~~the~~ industrial structure (Mi et al., 2017; Guan et al., 2018) and a decline in the share of coal used for energy (Qi et al., 2016). ~~S-and~~ strategies for reducing emissions could be based on such uniformed trends, while making reduction policies for provinces ~~needs-requires~~ the support of provincial ~~-energy-based~~ datasets instead of national ~~-energy-based ones~~ datasets.

Estimates with more sectors ~~would-are~~ usually higher than those with fewer ~~sectors~~. ~~For-In regard to the incorporation of~~ different emissions sectors, EDGAR ~~has-includes~~ international aviation and bunkers (Janssens-Maenhout et al., 2017) and NJU ~~has-incorporates~~ wastes sector (Liu et al., 2013) (Table S1), and thus, ~~both~~ were higher than ~~the~~ others. Moreover, for MEIC\_v.1.3 downloaded from ~~the~~ official website, ~~it-included~~ biofuel combustion (which accounted for ~~approximately~~ 5.7% of the total) ~~was included, and; however,~~ the version used here was specially prepared to exclude biofuel to increase ~~the database's~~ comparability ~~of the database~~. ~~For-another-instance~~ In addition, CEADs industry processes only ~~take-account~~ ~~of-include~~ cement production and was thus lower than those (e.g., NJU and EDGAR) ~~with-that include~~ more processes (iron and steel, etc.) (Janssens-Maenhout et al., 2017; Shan et al., 2018; Liu et al., 2013). ~~For-The~~ PKU dataset, ~~it~~ used IEA energy statistics with more detailed energy ~~sub-subtypes~~. The emissions factors ~~was-were~~ based on more detailed energy ~~sub-subtypes~~ with lower EFs, ~~and-while~~ other inventories used ~~the~~ averages of large groups (Table 1), ~~and-such that the~~ sum of more detailed ~~sub-subtypes~~ might not equal ~~to~~ the total of large groups due to ~~the~~ incompleteness of the statistics, ~~and~~ ~~These factors~~ could ~~be-explain the~~ reasons for ~~its-the~~ lower emissions estimate (Wang et al., 2013). A further comparison with IEA, EIA and BP estimates with only energy-related emissions also confirmed ~~ed~~ that estimates with more sectors would be ~~higher-greater~~ than those with fewer (Figure S1).

## 5.2 ~~Emission factor e~~ Effects of emission factors on the total emissions

Carbon emissions are calculated from activity data and EFs, and the uncertainty in estimates is typically reported as 5%—

360 -10%, while the maximum difference in this study reached 33.8% (or 2.7 PgC) in 2012. One major reason for this difference is the EF used by these inventories (Table 1). The EF for raw coal ranged from 0.491 to 0.746. For example, CEADs used 0.499 tC per ton of coal based on large-sample measurements, while EDGAR used 0.713 from the default values recommended by IPCC (Janssens-Maenhout et al., 2017; Liu et al., 2015b; Shan et al., 2018), and the differences ~~are were due~~ largely due to the low quality and high ash content of Chinese coal. The variability of lignite and coal quality is quite ~~largesignificant~~. In Liu et al. (2015), the carbon content of lignite ranged from 11% ~~to~~ 51%, with a mean  $\pm$ SD of 28%  $\pm$ 13 (n=61). Furthermore, another study showed that the uncertainty from EFs (-16% ~~to~~ -24%) was ~~much significantly higher~~ greater than that from activity data (-1% ~~to~~ 9%) (Shan et al., 2018). We recommended substituting the IPCC default coal EF with the CEADs EF. Regarding ~~the~~ plant-level emissions from coal consumptions, the collection of ~~their the~~ EFs measured at fields representing the quality and type of various coals ~~are is highly much~~ needed to calibrate the large point source emissions, and we call for the inclusion of physical measurements for the calibration and validation of existing datasets (Bai et al., 2007; Dai et al., 2012; Kittner et al., 2018; Yao et al., 2019). Different fuel types ~~would~~ contribute differently to emissions factors, i.e., for the same net heating value, natural gas emitted ~~lowest the least amount of~~ carbon dioxide (61.7 kg CO<sub>2</sub>/TJ energy), followed by oil (65.3 kg CO<sub>2</sub>/TJ energy) and coal (94.6 kg CO<sub>2</sub>/TJ energy), ~~and one~~. Similarly, one successful example for ~~reducing the reduction of~~ air pollutants and CO<sub>2</sub> was that the Chinese government initiated the “project of replacement of coal with natural gas and electricity in North China” in 2016 (Zheng et al., 2018a). Moreover, the non-oxidation fraction of 8% used in Liu et al. (2015) (Liu et al., 2015b) for coal was attributable to the differences when comparing with a default non-oxidation fraction of 0%, as recommended by IPCC (2006) in EDGAR (Janssens-Maenhout et al., 2017). Moreover, ~~the averaged~~ qualities of coal ~~qualities are varying vary~~ with time, yet we lacked such time-series quality data on raw coal. Bottom-up inventories typically use time-invariant EFs for CO<sub>2</sub> due to the lack of information on coal heating values over time; similarly, and the MEIC model also uses constant EFs of CO<sub>2</sub> (Zheng et al., 2018). Teng and Zhu (2015) recommended time-~~varied~~ conversion factors from raw coal to standard coal, ~~and as well as to~~ change the raw coal to commodity coal in energy balance statistics ~~since because~~ the latter has relatively efficient statistics on EF.

### 5.3 Spatial distribution of point, line and area sources

#### 5.3.1 Point sources in datasets and their effects on spatial distribution

385 Point sources emissions account for a large proportion of the total emissions (Hutchins et al., 2017). Power plants consumed ~~about approximately~~ half of the total coal production in the past decade (Liu et al., 2015a). Thus, the accuracy of point sources was extremely important for improving emission estimates. ODIAC, EDGAR, and PKU all distributed power plant emissions from the CARMA dataset. However, the geolocation errors in China are relatively large, and only 45% of power plants ~~were are~~ located in the same 0.1°  $\times$  0.1° grid in CARMA v2.0 as according to the real power plants locations that were   
390 identified by eyeballing visual inspection in google Google maps (Wang et al., 2013), ~~because. This discrepancy is due to the~~

~~fact that~~because CARMA generally treats ~~the~~ city-center latitudes and longitudes as the approximate coordinates of ~~the~~ power plants (Wheeler and Ummel, 2008;Ummel, 2012).

395 Liu et al. (2015a) found that CARMA neglected ~~about~~ approximately 1300 small power plants in China. Thus, CARMA allocated similar emissions to a more limited number of plants than CPED (Table S2, 720, 1706 and 2320 point sources for ODIAC, EDGAR and MEIC, respectively), and ODIAC had fewer point sources due to the elimination of ~~wrong~~ incorrect geolocations. The high-emitting grids in CHRED were attributed to the 1.58 million industrial enterprises from the First China Pollution Source Census (FCPSC) ~~that were~~ used as point sources (Wang et al., 2014). Following the CARMA example, we call on the open source of large point sources for datasets and reinforce the importance that Chinese scientists ~~need to~~ must adjust the locations of point sources from CARMA.

### 400 5.3.2 Effects of spatial disaggregation methods on line and area sources

Downscaling methods are widely used ~~for~~ because of its ~~their~~ uniformity and simplicity ~~because of the~~ due to the lack of detailed spatial data. The ~~d~~isaggregation methods used (e.g., nighttime light, population) by inventories strongly significantly affect the resulting spatial pattern. For example, ODIAC mainly uses nighttime light from satellite images to distribute emissions. Thus, the hotspots concentrated ~~more~~ in strongly in high nighttime light regions. However, ~~using the~~ use of remote sensing data ~~tend~~ se to underestimate industrial and transportation emissions (Ghosh et al., 2010). For instance, coal-fired power plants do not emit strong lights and may be far ~~away~~ from cities ~~by~~ because transmission lines are used. Electricity generation and use ~~are~~ usually ~~happened~~ at occur in different ~~places~~ locations, and stronger night-time light does not always ~~mean~~ indicate higher CO<sub>2</sub> emissions (Cai et al., 2018;Doll et al., 2000). Furthermore, night-time lights ~~would~~ ignore some other main fossil fuel emissions, such as household cooking with coal. The good correlation between night-time light and CO<sub>2</sub> emissions is usually on a larger scale basis (national or continental) (Oda et al., 2010;Raupach et al., 2010), while this relationship ~~would~~ fails in populated or industrialized rural areas.

Transport networks are also used in several inventories for spatial disaggregation. EDGAR and CHRED both showed clear transport emissions, especially in western China. EDGAR uses ~~se~~ three road types and their corresponding weighting factors to disaggregate line source emissions. CHRED uses ~~se~~ national traffic networks and their flows to distribute traffic emissions (Cai et al., 2018;Cai et al., 2012). It is easier to obtain ~~the~~ traffic networks but rather difficult to ~~get~~ obtain the traffic flows and vehicle kilometers travelled (VKT) data, and thus, the weighting factors method ~~are~~ is much significantly easier to apply. Population is widely used in spatial disaggregation (Andres et al., 2014;Andres et al., 2016;Janssens-Maenhout et al., 2017). ~~The~~ ODIAC emissions maps originally used ~~a~~ static population data to distribute emissions ~~and~~ but have recently have changed to a temporally varying population proxy, which has largely reduced ~~the~~ uncertainty. However, the unified algorithm for spatial disaggregation, such as the population density approach, ~~has~~ encounters difficulties in depicting the uneven development of rural and urban areas, and instead, it usually uses interpolation for a limited number of base years and does not truly vary across years at high spatial resolution (Andres et al., 2014). Furthermore, downscaling approaches may

introduce approximately 50% error per pixel, which are spatially correlated (Rayner et al., 2010), ~~and this problem needs to a problem which that must~~ be considered in future studies.

425 Moreover, big cities have virtually eliminated ~~the~~ use of coal (Guan et al., 2018; Zheng et al., 2018a), while in rural areas, the use of coal has even often increased (Meng et al., 2019). For example, a national survey showed that China's rural residential coal consumption fractions for heating increased from 19.2% to 27.2% (Tao et al., 2018). These transitions ~~has~~ have impacts on the spatial distribution of both CO<sub>2</sub> and air pollutants. ~~And In addition,~~ the high-resolution CO<sub>2</sub> emissions ~~have can serve as~~ a potential proxy for fossil fuel emissions (Wang et al., 2013); thus, further improvements ~~on to~~ spatial  
430 disaggregation should consider these transitions and the surveyed data.

*Data availability.* The data—sets of ODIAC, EDGAR, PKU and CEADs are freely available from  
435 <http://db.cger.nies.go.jp/dataset/ODIAC/>, [http://edgar.jrc.ec.europa.eu/overview.php?v=432\\_GHG&SECURE=123](http://edgar.jrc.ec.europa.eu/overview.php?v=432_GHG&SECURE=123),  
<http://inventory.pku.edu.cn/download/download.html> and <http://www.ceads.net/>—respectively, respectively. ~~And~~  
CHRED, MEIC and NJU are available from the data developers upon request.

*Author contributions.* PFH and NZ conceived and designed the study. PFH and XHL collected and analyzed the data  
440 sets. PFH, XHL, NZ and TO ~~led the paper writing wrote the paper~~, with contributions from all the coauthors.

*Competing interests.* The authors declare that they have no conflict of interest.

*Acknowledgments.* This work was supported by the National Key R&D Program of China (No. 2017YFB0504000). We  
445 thank Dr. Bofeng Cai from the Chinese Academy for Environmental Planning for kindly providing the CHRED data and  
his suggestions for improving the manuscript.

*Supporting Information.* Data and methodology descriptions ~~of a~~ the nine datasets and supplementary figures on  
emission estimates

## 450 **References**

- 451 Andres, R. J., Gregg, J. S., Losey, L., Marland, G., and Boden, T. A.: Monthly, global emissions of carbon  
452 dioxide from fossil fuel consumption, *Tellus*, 63, 309-327, 2011.
- 453 Andres, R. J., Boden, T. A., Bréon, F. M., and Ciais, P.: A synthesis of carbon dioxide emissions from  
454 fossil-fuel combustion, *Biogeosciences*, 9, 1845-1871, 2012.
- 455 Andres, R. J., Boden, T. A., and Higdon, D.: A new evaluation of the uncertainty associated with CDIAC  
456 estimates of fossil fuel carbon dioxide emission, *Tellus B: Chemical and Physical Meteorology*, 66,  
457 23616, 10.3402/tellusb.v66.23616, 2014.
- 458 Andres, R. J., Boden, T. A., and Higdon, D. M.: Gridded uncertainty in fossil fuel carbon dioxide  
459 emission maps, a CDIAC example, *Atmospheric Chemistry & Physics*, 16, 1-56, 2016.
- 460 Bai, X. F., Li, W. H., Chen, Y. F., and Jiang, Y.: The general distributions of trace elements in Chinese  
461 coals, *Coal Quality Technology*, 2007.
- 462 Bao, Z., Han, P., Zeng, N., Liu, D., Wang, Y., Tang, G., Yao, B., and Zheng, K.: Observation and modeling  
463 of vertical carbon dioxide distribution in a heavily polluted suburban environment, *Atmospheric and  
464 Oceanic Science Letters*, 10.1080/16742834.2020.1746627, 2020.
- 465 Berezin, E. V., Konovalov, I. B., Ciais, P., Richter, A., Tao, S., Janssens-Maenhout, G., Beekmann, M., and  
466 Schulze, E.-D.: Multiannual changes of CO<sub>2</sub> emissions in China: indirect estimates derived from  
467 satellite measurements of tropospheric NO<sub>2</sub> columns, *Atmos. Chem. Phys.*, 13, 9415-9438,  
468 <https://doi.org/9410.5194/acp-9413-9415-2013>, 2013.
- 469 Boden, T. A., Marland, G., and Andres, R. J.: Global, Regional, and National Fossil-Fuel CO<sub>2</sub> Emissions,  
470 Carbon Dioxide Information Analysis Center, Oak Ridge National Laboratory, U.S. Department of  
471 Energy, Oak Ridge, Tenn., USA, [https://doi.org/10.3334/CDIAC/00001\\_V2016](https://doi.org/10.3334/CDIAC/00001_V2016), in, 2016.
- 472 Byers, L., Friedrich, J., Hennig, R., Kressig, A., Li, X., McCormick, C., and Malaguzzi, V. L.: A Global  
473 Database of Power Plants, in, World Resources Institute. Available online at  
474 [www.wri.org/publication/global-database-power-plants](http://www.wri.org/publication/global-database-power-plants), Washington, DC, 2019.
- 475 Cai, B., Yang, W., Cao, D., Liu, L., Zhou, Y., and Zhang, Z.: Estimates of China's national and regional  
476 transport sector CO<sub>2</sub> emissions in 2007, *Energy Policy*, 41, 474-483, 2012.
- 477 Cai, B., Liang, S., Zhou, J., Wang, J., Cao, L., Qu, S., Xu, M., and Yang, Z.: China high resolution emission  
478 database (CHRED) with point emission sources, gridded emission data, and supplementary  
479 socioeconomic data, *Resources, Conservation and Recycling*, 129, 232-239,  
480 <https://doi.org/10.1016/j.resconrec.2017.10.036>, 2018.
- 481 Dai, S., Ren, D., Chou, C.-L., Finkelman, R. B., Seredin, V. V., and Zhou, Y.: Geochemistry of trace  
482 elements in Chinese coals: A review of abundances, genetic types, impacts on human health, and  
483 industrial utilization, *International Journal of Coal Geology*, 94, 3-21,  
484 <https://doi.org/10.1016/j.coal.2011.02.003>, 2012.
- 485 Doll, C. H., Muller, J.-P., and Elvidge, C. D.: Night-time Imagery as a Tool for Global Mapping of  
486 Socioeconomic Parameters and Greenhouse Gas Emissions, *AMBIO: A Journal of the Human  
487 Environment*, 29, 157-162, 10.1579/0044-7447-29.3.157, 2000.
- 488 Gately, C. K., Hutyrá, L. R., and Sue Wing, I.: Cities, traffic, and CO<sub>2</sub>: A multidecadal assessment of  
489 trends, drivers, and scaling relationships, *Proceedings of the National Academy of Sciences*, 112,  
490 4999-5004, 10.1073/pnas.1421723112, 2015.
- 491 Geofabrik: Openstreetmap, <https://www.openstreetmap.org> and OpenRailwayMap, 2015.

492 Ghosh, T., Elvidge, C. D., Sutton, P. C., Baugh, K. E., Ziskin, D., and Tuttle, B. T.: Creating a Global Grid of  
493 Distributed Fossil Fuel CO<sub>2</sub> Emissions from Nighttime Satellite Imagery, *Energies*, 3, 1895, 2010.

494 Guan, D., Liu, Z., Geng, Y., Lindner, S., and Hubacek, K.: The gigatonne gap in China's carbon dioxide  
495 inventories, *Nature Climate Change*, 2, 672-675, 10.1038/nclimate1560, 2012.

496 Guan, D., Meng, J., Reiner, D. M., Zhang, N., Shan, Y., Mi, Z., Shao, S., Liu, Z., Zhang, Q., and Davis, S. J.:  
497 Structural decline in China's CO<sub>2</sub> emissions through transitions in industry and energy systems, *Nature*  
498 *Geoscience*, 11, 551-555, 10.1038/s41561-018-0161-1, 2018.

499 Han, P., Lin, X., Zeng, N., Oda, T., Zhang, W., Liu, D., Cai, Q. C., Crippa, M., Guan, D., Ma, X.,  
500 Janssens-Maenhout, G., Meng, W., Shan, Y., Tao, S., Wang, G., Wang, H., Wang, R., Wu, L., Zhang, Q.,  
501 Zhao, F., and Zheng, B.: Province-level fossil fuel CO<sub>2</sub> emission estimates for China based on seven  
502 inventories (Accepted), *Journal of Cleaner Production*, 277, 10.1016/j.jclepro.2020.123377, 2020.

503 Hong, C., Zhang, Q., He, K., Guan, D., Li, M., Liu, F., and Zheng, B.: Variations of China's emission  
504 estimates: response to uncertainties in energy statistics, *Atmos. Chem. Phys.*, 17, 1227-1239,  
505 <https://doi.org/10.5194/acp-1217-1227-2017>, 2017.

506 Hutchins, M. G., Colby, J. D., Marland, G., and Marland, E.: A comparison of five high-resolution  
507 spatially-explicit, fossil-fuel, carbon dioxide emission inventories for the United States, *Mitigation and*  
508 *Adaptation Strategies for Global Change*, 22, 947.  
509 <https://doi.org/910.1007/s11027-11016-19709-11029>, 2017.

510 IEA: Energy Balances of OECD and non-OECD countries, International Energy Agency, Paris, Beyond  
511 2020 Online Database, in, 2014.

512 IPCC: IPCC Guidelines for National Greenhouse Gas Inventories. Eggleston, S., Buendia, L., Miwa, K.,  
513 Ngara, T., Tanabe, K. (eds.). , IPCC-TSU NGGIP, IGES, Hayama, Japan.  
514 [www.ipcc-nggip.iges.or.jp/public/2006gl/index.html](http://www.ipcc-nggip.iges.or.jp/public/2006gl/index.html), 2007.

515 IPCC AR5: IPCC 2013: the physical science basis. Contribution of Working Group I to the Fifth  
516 Assessment Report of the Intergovernmental Panel on Climate Change, in, edited by: Stocker, T., Qin,  
517 D., Plattner, G., Tignorand, M., Allen, S., Boschungand, J., Nauels, A., Xia, Y., Bex, V., and Midgley, P.,  
518 Cambridge University Press, Cambridge, UK, 2013.

519 Janssens-Maenhout, G., Crippa, M., Guizzardi, D., Muntean, M., Schaaf, E., Dentener, F., Bergamaschi,  
520 P., Pagliari, V., Olivier, J. G. J., Peters, J. A. H. W., van Aardenne, J. A., Monni, S., Doering, U., and  
521 Petrescu, A. M. R.: EDGAR v4.3.2 Global Atlas of the three major Greenhouse Gas Emissions for the  
522 period 1970–2012, *Earth Syst. Sci. Data Discuss.*, <https://doi.org/10.5194/essd-2017-5179>, 2017.

523 Janssens-Maenhout, G., Crippa, M., Guizzardi, D., Muntean, M., Schaaf, E., Dentener, F., Bergamaschi,  
524 P., Pagliari, V., Olivier, J. G., and Peters, J. A.: EDGAR v4. 3.2 Global Atlas of the three major greenhouse  
525 gas emissions for the period 1970–2012, *Earth System Science Data*, 11, 959-1002, 2019a.

526 Janssens-Maenhout, G., Crippa, M., Guizzardi, D., Muntean, M., Schaaf, E., Dentener, F., Bergamaschi,  
527 P., Pagliari, V., Olivier, J. G. J., Peters, J. A. H. W., van Aardenne, J. A., Monni, S., Doering, U., Petrescu, A.  
528 M. R., Solazzo, E., and Oreggioni, G. D.: EDGAR v4.3.2 Global Atlas of the three major greenhouse gas  
529 emissions for the period 1970–2012, *Earth Syst. Sci. Data*, 11, 959-1002, 10.5194/essd-11-959-2019,  
530 2019b.

531 Kittner, N., Fadadu, R. P., Buckley, H. L., Schwarzman, M. R., and Kammen, D. M.: Trace Metal Content  
532 of Coal Exacerbates Air-Pollution-Related Health Risks: The Case of Lignite Coal in Kosovo,  
533 *Environmental Science & Technology*, 52, 2359-2367, 10.1021/acs.est.7b04254, 2018.

534 Le Quéré, C., Andrew, R. M., Friedlingstein, P., Sitch, S., Pongratz, J., Manning, A. C., Korsbakken, J. I.,  
535 Peters, G. P., Canadell, J. G., Jackson, R. B., Boden, T. A., Tans, P. P., Andrews, O. D., Arora, V. K., Bakker,

536 D. C. E., Barbero, L., Becker, M., Betts, R. A., Bopp, L., Chevallier, F., Chini, L. P., Ciais, P., Cosca, C. E.,  
537 Cross, J., Currie, K., Gasser, T., Harris, I., Hauck, J., Haverd, V., Houghton, R. A., Hunt, C. W., Hurtt, G.,  
538 Ilyina, T., Jain, A. K., Kato, E., Kautz, M., Keeling, R. F., Klein Goldewijk, K., Körtzinger, A., Landschützer,  
539 P., Lefèvre, N., Lenton, A., Lienert, S., Lima, I., Lombardozzi, D., Metzl, N., Millero, F., Monteiro, P. M. S.,  
540 Munro, D. R., Nabel, J. E. M. S., Nakaoka, S.-I., Nojiri, Y., Padin, X. A., Peregón, A., Pfeil, B., Pierrot, D.,  
541 Poulter, B., Rehder, G., Reimer, J., Rödenbeck, C., Schwinger, J., Séférian, R., Skjelvan, I., Stocker, B. D.,  
542 Tian, H., Tilbrook, B., Tubiello, F. N., van der Laan-Luijkx, I. T., van der Werf, G. R., van Heuven, S., Viovy,  
543 N., Vuichard, N., Walker, A. P., Watson, A. J., Wiltshire, A. J., Zaehle, S., and Zhu, D.: Global Carbon  
544 Budget 2017, *Earth Syst. Sci. Data*, 10, 405-448, <https://doi.org/410.5194/essd-5110-5405-2018>, 2018.  
545 Lei, Y., Zhang, Q., Nielsen, C., and He, K.: An inventory of primary air pollutants and CO<sub>2</sub> emissions  
546 from cement production in China, 1990–2020, *Atmospheric Environment*, 45, 147-154,  
547 <https://doi.org/10.1016/j.atmosenv.2010.09.034>, 2011.  
548 Li, M., Zhang, Q., Kurokawa, J.-I., Woo, J.-H., He, K., Lu, Z., Ohara, T., Song, Y., Streets, D. G., Carmichael,  
549 G. R., Cheng, Y., Hong, C., Huo, H., Jiang, X., Kang, S., Liu, F., Su, H., and Zheng, B.: MIX: a mosaic Asian  
550 anthropogenic emission inventory under the international collaboration framework of the MICS-Asia  
551 and HTAP, *Atmos. Chem. Phys.*, 17, 2017.  
552 Liu, F., Zhang, Q., Tong, D., Zheng, B., Li, M., Huo, H., and He, K. B.: High-resolution inventory of  
553 technologies, activities, and emissions of coal-fired power plants in China from 1990 to 2010, *Atmos.*  
554 *Chem. Phys.*, 15, 13299-13317, 2015a.  
555 Liu, M., Wang, H., Oda, T., Zhao, Y., Yang, X., Zang, R., Zang, B., Bi, J., and Chen, J.: Refined estimate of  
556 China's CO<sub>2</sub> emissions in spatiotemporal distributions, *Atmos. Chem. Phys.*, 13, 10873-10882,  
557 <https://doi.org/10810.15194/acp-10813-10873-12013>, 2013.  
558 Liu, Z., Guan, D., Wei, W., Davis, S. J., Ciais, P., Bai, J., Peng, S., Zhang, Q., Hubacek, K., Marland, G.,  
559 Andres, R. J., Crawford-Brown, D., Lin, J., Zhao, H., Hong, C., Boden, T. A., Feng, K., Peters, G. P., Xi, F.,  
560 Liu, J., Li, Y., Zhao, Y., Zeng, N., and He, K.: Reduced carbon emission estimates from fossil fuel  
561 combustion and cement production in China, *Nature*, 524, 335, [10.1038/nature14677](https://doi.org/10.1038/nature14677)  
562 <https://www.nature.com/articles/nature14677#supplementary-information>, 2015b.  
563 Marland, G., Hamal, K., and Jonas, M.: How Uncertain Are Estimates of CO<sub>2</sub> Emissions?, *Journal of*  
564 *Industrial Ecology*, 13, 4-7, 2010.  
565 Meng, W., Zhong, Q., Chen, Y., Shen, H., Yun, X., Smith, K. R., Li, B., Liu, J., Wang, X., Ma, J., Cheng, H.,  
566 Zeng, E. Y., Guan, D., Russell, A. G., and Tao, S.: Energy and air pollution benefits of household fuel  
567 policies in northern China, *Proceedings of the National Academy of Sciences*, 116, 16773,  
568 [10.1073/pnas.1904182116](https://doi.org/10.1073/pnas.1904182116), 2019.  
569 Mi, Z., Meng, J., Guan, D., Shan, Y., Liu, Z., Wang, Y., Feng, K., and Wei, Y.-M.: Pattern changes in  
570 determinants of Chinese emissions, *Environmental Research Letters*, 12, 074003,  
571 [10.1088/1748-9326/aa69cf](https://doi.org/10.1088/1748-9326/aa69cf), 2017.  
572 National Bureau of Statistics: China Statistical Yearbook 1998–2016, China Statistics Press, 1998–2017.  
573 National Bureau of Statistics: China Energy Statistical Yearbook 2016, China Statistics Press, Beijing,  
574 2016.  
575 NDRC: The People's Republic of China Second National Communication on Climate Change,  
576 <http://ghs.ndrc.gov.cn/zcfg/201404/W020140415316896599816.pdf>, 2012a.  
577 NDRC: Guidelines for China's Provincial GHG Emission Inventories, in, 2012b.  
578 Oda, T., Maksyutov, S., and Elvidge, C. D.: Disaggregation of national fossil fuel CO<sub>2</sub> emissions using a  
579 global power plant database and DMSP nightlight data, *Proc. of the 30th Asia-Pacific Advanced*



580 Network Meeting, 220–229, 2010.

581 Oda, T., and Maksyutov, S.: A very high-resolution (1 km×1 km) global fossil fuel CO<sub>2</sub> emission  
582 inventory derived using a point source database and satellite observations of nighttime lights, *Atmos.*  
583 *Chem. Phys.*, 11, 543-556, <https://doi.org/510.5194/acp-5111-5543-2011>, 2011.

584 Oda, T., Maksyutov, S., and Andres, R. J.: The Open-source Data Inventory for Anthropogenic CO<sub>2</sub>,  
585 version 2016 (ODIAC2016): a global monthly fossil fuel CO<sub>2</sub> gridded emissions data product for tracer  
586 transport simulations and surface flux inversions, *Earth Syst. Sci. Data*, 10, 87-107,  
587 <https://doi.org/110.5194/essd-5110-5187-2018>, 2018.

588 Olivier, J. G. J., Janssens - Maenhout, G., Muntean, M., and Peters, J. A. H. W.: Trends in global CO<sub>2</sub>  
589 emissions: 2014 report, JRC93171/PBL1490 report, ISBN: 978-994-91506-91587-91501, 2014.

590 Qi, Y., Stern, N., Wu, T., Lu, J., and Green, F.: China's post-coal growth, *Nature Geoscience*, 9, 564-566,  
591 10.1038/ngeo2777, 2016.

592 Qin, D., Ding, Y., and Mu, M.: Climate and Environmental Change in China: 1951–2012, in: Springer  
593 Environmental Science & Engineering, edited by: Qin, D., Ding, Y., and Mu, M., Springer-Verlag Berlin  
594 Heidelberg 2016, 2016.

595 Raupach, M. R., Rayner, P. J., and Paget, M.: Regional variations in spatial structure of nightlights,  
596 population density and fossil-fuel CO<sub>2</sub> emissions, *Energy Policy*, 38, 4756-4764,  
597 <https://doi.org/10.1016/j.enpol.2009.08.021>, 2010.

598 Rayner, P. J., Raupach, M. R., Paget, M., Peylin, P., and Koffi, E.: A new global gridded data set of CO<sub>2</sub>  
599 emissions from fossil fuel combustion: Methodology and evaluation, *Journal of Geophysical Research*  
600 *Atmospheres*, 115, doi:10.1029/2009JD013439, 2010.

601 SCIO, T. S. C. I. O. o. C.: Enhanced Actions on Climate Change: China's Intended Nationally Determined  
602 Contributions,  
603 [http://www.scio.gov.cn/xwfbh/xwfbh/wqfbh/33978/35364/xgzc35370/Document/1514539/1514539](http://www.scio.gov.cn/xwfbh/xwfbh/wqfbh/33978/35364/xgzc35370/Document/1514539/1514539.htm)  
604 [9.htm](http://www.scio.gov.cn/xwfbh/xwfbh/wqfbh/33978/35364/xgzc35370/Document/1514539/1514539.htm), 2015.

605 Shan, Y., Liu, J., Liu, Z., Xu, X., Shao, S., Wang, P., and Guan, D.: New provincial CO<sub>2</sub> emission  
606 inventories in China based on apparent energy consumption data and updated emission factors,  
607 *Applied Energy*, 184, 2016.

608 Shan, Y., Guan, D., Zheng, H., Ou, J., Li, Y., Meng, J., Mi, Z., Liu, Z., and Zhang, Q.: China CO<sub>2</sub> emission  
609 accounts 1997-2015, *Scientific Data*, 5, 170201, 2018.

610 Tao, S., Ru, M. Y., Du, W., Zhu, X., Zhong, Q. R., Li, B. G., Shen, G. F., Pan, X. L., Meng, W. J., Chen, Y. L.,  
611 Shen, H. Z., Lin, N., Su, S., Zhuo, S. J., Huang, T. B., Xu, Y., Yun, X., Liu, J. F., Wang, X. L., Liu, W. X., Cheng,  
612 H. F., and Zhu, D. Q.: Quantifying the rural residential energy transition in China from 1992 to 2012  
613 through a representative national survey, *Nature Energy*, 3, 567-573, 10.1038/s41560-018-0158-4,  
614 2018.

615 Teng, F., and Zhu, S.: Which estimation is more accurate? A technical comments on Nature Paper by  
616 Liu et al on overestimation of China's emission, *Science & Technology Review*, 33, 112-116, 2015.

617 Ummel, K.: Carma Revisited: An Updated Database of Carbon Dioxide Emissions from Power Plants  
618 Worldwide, Working Papers, 2012.

619 Wang, J., Cai, B., Zhang, L., Cao, D., Liu, L., Zhou, Y., Zhang, Z., and Xue, W.: High resolution carbon  
620 dioxide emission gridded data for China derived from point sources, *Environmental Science &*  
621 *Technology*, 48, 7085-7093, 2014.

622 Wang, M., and Cai, B.: A two-level comparison of CO<sub>2</sub> emission data in China: Evidence from three  
623 gridded data sources, *Journal of Cleaner Production*, 148, 194-201,

624 <https://doi.org/10.1016/j.jclepro.2017.02.003>, 2017.

625 Wang, R., Tao, S., Ciais, P., Shen, H. Z., Huang, Y., Chen, H., Shen, G. F., Wang, B., Li, W., Zhang, Y. Y., Lu,  
626 Y., Zhu, D., Chen, Y. C., Liu, X. P., Wang, W. T., Wang, X. L., Liu, W. X., Li, B. G., and Piao, S. L.:  
627 High-resolution mapping of combustion processes and implications for CO<sub>2</sub> emissions, *Atmos. Chem.*  
628 *Phys.*, 13, 5189-5203, <https://doi.org/5110.5194/acp-5113-5189-2013>, 2013.

629 Wheeler, D., and Ummel, K.: Calculating CARMA: Global Estimation of CO<sub>2</sub> Emissions from the Power  
630 Sector, Working Papers, 2008.

631 Yao, B., Cai, B., Kou, F., Yang, Y., Chen, X., Wong, D. S., Liu, L., Fang, S., Liu, H., Wang, H., Zhang, L., Li, J.,  
632 and Kuang, G.: Estimating direct CO<sub>2</sub> and CO emission factors for industrial rare earth metal  
633 electrolysis, *Resources, Conservation and Recycling*, 145, 261-267,  
634 <https://doi.org/10.1016/j.resconrec.2019.02.019>, 2019.

635 Zeng, N., Ding, Y., Pan, J., Wang, H., and Gregg, J.: Climate Change--the Chinese Challenge, *Science*,  
636 319, 730-731, 10.1126/science.1153368, 2008.

637 Zhang, Q., Streets, D. G., He, K., and Klimont, Z.: Major components of China's anthropogenic primary  
638 particulate emissions, *Environmental Research Letters*, 2, 045027, 2007.

639 Zheng, B., Zhang, Q., Tong, D., Chen, C., Hong, C., Li, M., Geng, G., Lei, Y., Huo, H., and He, K.:  
640 Resolution dependence of uncertainties in gridded emission inventories: a case study in Hebei, China,  
641 *Atmos. Chem. Phys.*, 17, <https://doi.org/10.5194/acp-17-921-2017>, 2017.

642 Zheng, B., Tong, D., Li, M., Liu, F., Hong, C., Geng, G., Li, H., Li, X., Peng, L., Qi, J., Yan, L., Zhang, Y., Zhao,  
643 H., Zheng, Y., He, K., and Zhang, Q.: Trends in China's anthropogenic emissions since 2010 as the  
644 consequence of clean air actions, *Atmos. Chem. Phys.*, 18, 14095-14111,  
645 <https://doi.org/14010.15194/acp-14018-14095-12018>, , 2018a.

646 Zheng, B., Zhang, Q., Davis, S. J., Ciais, P., Hong, C., Li, M., Liu, F., Tong, D., Li, H., and He, K.:  
647 Infrastructure Shapes Differences in the Carbon Intensities of Chinese Cities, *Environmental Science &*  
648 *Technology*, 52, 6032-6041, 10.1021/acs.est.7b05654, 2018b.

649

650